

On the identity of the identity operator in nonadiabatic linearized semiclassical dynamics

Maximilian A. C. Saller,¹ Aaron Kelly,² and Jeremy O. Richardson^{1, a)}

¹⁾Laboratory of Physical Chemistry, ETH Zurich, 8093 Zurich, Switzerland

²⁾Department of Chemistry, Dalhousie University, B3H 4R2 Halifax, Canada

(Dated: 22 November 2018)

Simulating the nonadiabatic dynamics of condensed-phase systems continues to pose a significant challenge for quantum dynamics methods. Approaches based on sampling classical trajectories within the mapping formalism, such as the linearized semiclassical initial value representation (LSC-IVR), can be used to approximate quantum correlation functions in dissipative environments. Such semiclassical methods however commonly fail in quantitatively predicting the electronic-state populations in the long-time limit. Here we present a suggestion to minimize this difficulty by splitting the problem into two parts, one of which involves the identity, and treating this operator by quantum-mechanical principles rather than with classical approximations. This strategy is applied to numerical simulations of spin-boson model systems, showing its potential to drastically improve the performance of LSC-IVR and related methods with no change to the equations of motion or the algorithm in general, but rather by simply using different functional forms of the observables.

I. INTRODUCTION

The study of nonadiabatic processes in condensed-phase systems remains a challenge for computer simulation. These phenomena, occurring when two or more states approach each other in energy, influence a wide variety of systems in physics, chemistry and biology.¹⁻⁴

Significant efforts continue to be devoted to the development of quantum dynamics methods which can accurately capture nonadiabatic effects. While grid-based wavefunction propagation shows considerable promise for small or model systems,⁵⁻⁸ many realistic problems are simply too large and complex to treat with such approaches, given their unfavourable exponential scaling with system size. Despite progress in methodology relying, in part, on classical trajectories,^{9,10} more approximate semiclassical techniques are generally required in the condensed phase.¹¹⁻¹⁷ Their favourable, linear scaling with system size allows insight into realistic processes to be gained without incurring extreme computational costs.

A typical nonadiabatic process may be described by a continuous nuclear phase space and a discrete electronic state space. The total Hamiltonian is given by

$$\hat{H} = \sum_{j=1}^F \frac{\hat{p}_j^2}{2m_j} + U(\hat{x}) + \hat{V}(\hat{x}), \quad (1)$$

where x and p are F -dimensional vectors containing the position and momenta for each nuclear degree of freedom with masses m_j . $U(x)$ is the state-independent potential and, for the case of two electronic states, the state-dependent potential is

$$\hat{V}(x) = V_1(x) |1\rangle\langle 1| + V_2(x) |2\rangle\langle 2| + \Delta(x) (|1\rangle\langle 2| + |2\rangle\langle 1|), \quad (2)$$

where $V_1(x)$ and $V_2(x)$ are the potential-energy surfaces of diabatic states $|1\rangle$ and $|2\rangle$ and $\Delta(x)$ is the coupling between the states. While written and presented in the context of two electronic states here, all aspects of this work can be generalized to any number of electronic states. Reduced units will be employed throughout, such that $\hbar = 1$.

The aforementioned issue of mismatched discrete and continuous spaces clearly arises from the final term in Eq. 1. In order to express the problem in terms of continuous variables, the electronic states can be mapped onto a space of singly-excited harmonic oscillators (SEOs).¹⁸ Projecting into the space of the SEOs yields the wavefunction

$$\langle X|n\rangle = \sqrt{\frac{2}{\pi}} X_n e^{-(X_1^2 + X_2^2)/2} \quad (3)$$

in terms of positions, X , or equivalently momenta, P , which are 2-dimensional vectors known as mapping variables. This allows the entire system to be described *via* an extended phase space, $\{x, p, X, P\}$, which can be sampled and explored using classical trajectories.^{19,20} The classical Hamiltonian underlying the mapping approach is given by

$$\mathcal{H} = \sum_{j=1}^F \frac{p_j^2}{2m_j} + U(x) + \frac{1}{2} [X^T V X + P^T V P - \text{tr} V], \quad (4)$$

where V is the matrix representation of $\hat{V}(x)$.

Owing to the relative simplicity of the mapping approach and the convenience of being able to describe the total system in terms of an extended phase space that grows only linearly with the number of nuclear degrees of freedom and electronic states, a considerable number of approaches have been developed with it at their core.¹⁸⁻³⁹

Many semiclassical nonadiabatic simulation methods struggle in predicting the correct long-time limit of observables for asymmetric systems. One suggestion for improving the accuracy has been to utilize the formalism of

^{a)}Electronic mail: jeremy.richardson@phys.chem.ethz.ch

master equations.⁴⁰ The benefits of this include a noticeable gain in accuracy as well as the ability to obtain long time dynamics using only short time trajectories.^{41–44} A similar motivation underlies the approach presented here, albeit using a simpler strategy. First we recast the observable of interest in terms of a correlation function involving the identity operator. In quantum mechanics, the effect of the identity operator is known to be exactly unity. The classical equivalent of this operation is clearly to multiply by the number one. We therefore calculate the correlation function with this definition of the identity, instead of using the approximation provided by the semiclassical trajectories. The result is a marked improvement in accuracy.

II. THEORY

In this section we present the formalism for evaluating correlation functions using semiclassical methods and consider the various options for classical representations of the quantum operators.

A. Linearized semiclassical initial value representation

In the study of condensed-phase systems, the quantity of interest can typically be expressed as a time correlation function between two quantum operators, \hat{A} and \hat{B} , given by

$$C_{AB}(t) = \text{Tr} \left[\hat{\rho} \hat{A} e^{i\hat{H}t} \hat{B} e^{-i\hat{H}t} \right], \quad (5)$$

where $\hat{\rho}$ is the initial density matrix, normalized such that $\text{Tr}[\hat{\rho}] = 1$.

In order to take the semiclassical approximation, it is necessary to rewrite the correlation function in terms of the mapping variables. This is readily achieved using the Wigner transform, given, for any general quantum operator, \hat{O} , by

$$\mathcal{O}^w(x, p, \mathbf{X}, \mathbf{P}) = \iint e^{ip \cdot y + i\mathbf{P} \cdot \mathbf{Y}} \left\langle x - \frac{y}{2}, \mathbf{X} - \frac{\mathbf{Y}}{2} \left| \hat{O} \right| x + \frac{y}{2}, \mathbf{X} + \frac{\mathbf{Y}}{2} \right\rangle dy d\mathbf{Y}, \quad (6)$$

where y and \mathbf{Y} are dummy variables of the same shape as x and \mathbf{X} . Using this phase-space representation, the exact quantum correlation function can be written as

$$C_{AB}(t) = \frac{1}{(2\pi)^{F+L}} \iiint \left[\hat{\rho} \hat{A} \right]^w(x, p, \mathbf{X}, \mathbf{P}) \left[\hat{B}(t) \right]^w(x, p, \mathbf{X}, \mathbf{P}) dx dp d\mathbf{X} d\mathbf{P}. \quad (7)$$

No approximation has been made, and in this expression the time-dependent operator $\hat{B}(t) \equiv e^{i\hat{H}t} \hat{B} e^{-i\hat{H}t}$ has to be computed by quantum-mechanical propagation. In cases, such as the ones studied here, where the density matrix, $\hat{\rho}$, and the operator \hat{A} commute,

the Wigner transform of the product, $[\hat{\rho} \hat{A}]^w(x, p, \mathbf{X}, \mathbf{P}) \equiv \rho^w(x, p, \mathbf{X}, \mathbf{P}) A^w(x, p, \mathbf{X}, \mathbf{P})$, may be used instead.

An approximation to the correlation function is obtained if classical trajectories defined by the mapping Hamiltonian of Eq. 4, are employed to determine the value of the Wigner-transformed operator at time t .⁴⁵ This gives

$$C_{AB}(t) \approx \frac{1}{(2\pi)^{F+L}} \iiint \rho^w(x, p, \mathbf{X}, \mathbf{P}) A^w(x, p, \mathbf{X}, \mathbf{P}) B^w(x(t), p(t), \mathbf{X}(t), \mathbf{P}(t)) dx dp d\mathbf{X} d\mathbf{P}. \quad (8)$$

This expression is known in the literature as the linearized semiclassical initial value representation (LSC-IVR).²² Notably, the approximation in Eq. 8 is exact at $t = 0$ but depending on the problem may give poor results in the long-time limit.

B. Pauli spin operators

Many nonadiabatic processes of interest occur between two electronic states. This includes for example electron-transfer reactions^{1,2} and dynamics near conical intersections.³ In general, all operators relevant to a two-state quantum system can be written in terms of the traceless Pauli spin matrices, $\hat{\sigma}_x$, $\hat{\sigma}_y$ and $\hat{\sigma}_z$, and the identity, \hat{I} . Employing the mapping approach allows these operators to be expressed as¹⁸

$$\hat{\sigma}_x = |2\rangle\langle 1| + |1\rangle\langle 2| \mapsto \hat{X}_1 \hat{X}_2 + \hat{P}_1 \hat{P}_2 \quad (9a)$$

$$\hat{\sigma}_y = i(|2\rangle\langle 1| - |1\rangle\langle 2|) \mapsto \hat{X}_1 \hat{P}_2 - \hat{P}_1 \hat{X}_2 \quad (9b)$$

$$\hat{\sigma}_z = |1\rangle\langle 1| - |2\rangle\langle 2| \mapsto \frac{1}{2}(\hat{X}_1^2 + \hat{P}_1^2 - \hat{X}_2^2 - \hat{P}_2^2) \quad (9c)$$

$$\hat{I} = |1\rangle\langle 1| + |2\rangle\langle 2| \mapsto \frac{1}{2}(\hat{X}_1^2 + \hat{P}_1^2 + \hat{X}_2^2 + \hat{P}_2^2 - 2). \quad (9d)$$

In order to calculate LSC-IVR correlation functions *via* Eq. 8, these operators must be Wigner transformed to yield phase-space representations in terms of the mapping variables, \mathbf{X} and \mathbf{P} , which can be evolved with classical trajectories.

For each of these operators, there are two possible forms of the Wigner transform, one which is projected onto the SEO subspace, and one which is not.²⁰ Wigner transforming the operators in the form given on the right-hand sides of Eqs. 9, *i.e.* without projecting into the SEO subspace, yields phase-space representations of the same functional form in terms of the mapping variables, *e.g.*

$$\sigma_z^w(\mathbf{X}, \mathbf{P}) = \frac{1}{2} (X_1^2 + P_1^2 - X_2^2 - P_2^2) \quad (10a)$$

$$\mathcal{I}^w(\mathbf{X}, \mathbf{P}) = \frac{1}{2} (X_1^2 + P_1^2 + X_2^2 + P_2^2 - 2). \quad (10b)$$

On the other hand, taking the Wigner transform of the state-state representation and using the SEO projection, Eq. 3, yields

$$\sigma_\alpha^{\text{SEO}}(\mathbf{X}, \mathbf{P}) = \sigma_\alpha^w \phi \quad \alpha \in \{x, y, z\} \quad (11a)$$

$$\mathcal{I}^{\text{SEO}}(\mathbf{X}, \mathbf{P}) = \tilde{\mathcal{I}} \phi, \quad (11b)$$

where

$$\tilde{\mathcal{I}} = \frac{1}{2} (X_1^2 + P_1^2 + X_2^2 + P_2^2 - 1), \quad (12)$$

and

$$\phi = 16 \exp(-X_1^2 - X_2^2 - P_1^2 - P_2^2). \quad (13)$$

Note that unlike for the Pauli spin operators, the projected Wigner function \mathcal{I}^{SEO} is not simply equal to its unprojected form, \mathcal{I}^{w} , multiplied by ϕ .

C. Observables and Correlation functions

In two-state quantum systems, a quantity of particular interest is the population difference between the two states, $P(t)$, measured by the operator $\hat{\sigma}_z$. A commonly studied,^{41–43,46} non-equilibrium initial condition is a separable bath thermal density with the system purely in one electronic state, *i.e.* $\hat{\rho}_{\text{b}} |1\rangle\langle 1|$. This is normalized such that its trace is unity.

In this case, the population difference is given by

$$P(t) = \text{Tr}[\hat{\rho}_{\text{b}} |1\rangle\langle 1| \hat{\sigma}_z(t)] \quad (14a)$$

$$= C_{\mathcal{I}\sigma_z}(t) + C_{\sigma_z\sigma_z}(t), \quad (14b)$$

where the normalized density matrix appearing in the correlation functions is $\hat{\rho} = \hat{\rho}_{\text{b}}/2$. These two expressions are identical because $(\tilde{\mathcal{I}} + \hat{\sigma}_z)/2 = |1\rangle\langle 1|$, and we have simply separated the operator into trace-containing and traceless parts for clarity in what follows.

By considering known relations of the Pauli matrices, one can show that $C_{\sigma_z\sigma_z}(t)$ has an initial value of one and decays to zero in the long-time limit. $C_{\mathcal{I}\sigma_z}(t)$ on the other hand, starts at zero and plateaus at long times to a system-dependent finite value. Notably most semiclassical approximations, including LSC-IVR, capture the short time behaviour of these two correlation functions and for symmetry reasons the long-time decay of $C_{\sigma_z\sigma_z}(t)$ to zero as well. It is however much more difficult to obtain an accurate quantitative prediction of the long-time limit of $C_{\mathcal{I}\sigma_z}(t)$.

As a result of the different forms of the Wigner functions, there are number of ways in which the LSC-IVR correlation function could be evaluated, and in general they will give different approximations. Note that in order to ensure that the mapping variables describe the physical system, it is necessary for at least one of the operators to be projected onto the SEO subspace.

As shown in Eq. 9d there exists an expression for the identity operator in terms of the mapping variables. According to quantum mechanics, this operator measures the total population of the system and should always return exactly unity. However, it is known that the classical trajectories do not obey this rule correctly, and this is one of the main sources of error in the approximation.^{20,26,36} We propose that some of the errors associated with this can be eliminated by invoking the exact nature of the

TABLE I. Different formulations of the LSC-IVR correlation function, as shown in Eq. 8. We define $\rho^{\text{w}} = \rho_{\text{b}}^{\text{w}} \rho_{\text{el}}^{\text{w}}/2$.

method	$\rho_{\text{el}}^{\text{w}}(X, P)$	$C_{\mathcal{I}\sigma_z}(t)$		$C_{\sigma_z\sigma_z}(t)$	
		A^{w}	B^{w}	A^{w}	B^{w}
“double unity”	ϕ^2	1	σ_z^{w}	σ_z^{w}	σ_z^{w}
“double SEO”	ϕ^2	$\tilde{\mathcal{I}}$	σ_z^{w}	σ_z^{w}	σ_z^{w}
“single unity”	ϕ	1	σ_z^{w}	σ_z^{w}	σ_z^{w}
“single Wigner”	ϕ	\mathcal{I}^{w}	σ_z^{w}	σ_z^{w}	σ_z^{w}
“single SEO”	ϕ	$\tilde{\mathcal{I}}$	σ_z^{w}	σ_z^{w}	σ_z^{w}

identity operator. In practice this is achieved by simply replacing the mapping representation of the identity with the number 1 when calculating correlation functions.

Table I shows the different formulations of the LSC-IVR correlation functions that are employed here. The terms “single” and “double” refer to whether only one, or both operators are projected into the SEO subspace. “Unity”, “SEO” and “Wigner” are used to identify what functional form of the identity operator is used. There are thus five distinct LSC-IVR approximations for $C_{\mathcal{I}\sigma_z}(t)$. However, there are only two possibilities for $C_{\sigma_z\sigma_z}(t)$, using either “single” or “double” projections. Note that, as the function ϕ is time-independent under dynamics of \mathcal{H} , we have chosen to include it explicitly in the formulation of the density matrix, $\rho^{\text{w}} = \rho_{\text{b}}^{\text{w}} \rho_{\text{el}}^{\text{w}}/2$, which defines the sampling distribution of initial conditions.²²

Our approach is therefore to compute $P(t)$ via two correlation functions, as defined in Eq. 14b. We employ the LSC-IVR approximation, Eq. 8, for each correlation function using the functions defined in Table I. Both correlation functions can be evaluated by a single simulation, and in fact since the B^{w} functions are the same in each case, one could equivalently add the two A^{w} functions together to give a single correlation function. The standard LSC-IVR approach advocated in Ref. 22 is equivalent to the “double SEO” approach. It uses $A^{\text{w}} = \tilde{\mathcal{I}} + \sigma_z^{\text{w}} = X_1^2 + P_1^2 - \frac{1}{2}$, $B^{\text{w}} = \sigma_z^{\text{w}}$ and $\rho_{\text{el}}^{\text{w}} = \phi^2$. In our tests, this is actually one of the least accurate of the approaches defined in the table. The Poisson-bracket mapping equation (PBME) approach described in Ref. 24 on the other hand corresponds to “single SEO”, which is the same except for the sampling distribution $\rho_{\text{el}}^{\text{w}} = \phi$. The formulation which we find to be most accurate is “double unity”, which is equivalent to using $A^{\text{w}} = 1 + \sigma_z^{\text{w}}$ with $\rho_{\text{el}}^{\text{w}} = \phi^2$.

III. RESULTS AND DISCUSSION

In order to test the accuracy of the various approaches proposed here, we perform numerical simulations on the spin-boson model and compare the predicted time-dependent population difference with exact results.

A. The spin-boson Hamiltonian

The spin-boson Hamiltonian serves as a simple, yet challenging model which incorporates the key aspects of dissipative quantum systems.^{47–49} Owing to the wide variety of dynamical regimes accessible *via* its relatively few parameters, it has been thoroughly studied, and exact results are available^{50–53} to serve as a benchmark for new quantum dynamics methods.^{23–25,27,37,40–45}

The spin-boson model is a two-state quantum system, coupled to a bath of harmonic oscillators. In the context of the general Hamiltonian given in Eq. 1, it is defined by

$$\hat{V}(x) = \varepsilon \hat{\sigma}_z + \Delta \hat{\sigma}_x + \sum_{j=1}^F c_j x_j \hat{\sigma}_z \quad (15a)$$

$$U(x) = \frac{1}{2} \sum_{j=1}^F m_j \omega_j^2 x_j^2, \quad (15b)$$

where ε and Δ are the energy bias and constant diabatic coupling between the two electronic states forming the quantum system. The j th nuclear degree of freedom has frequency ω_j and vibronic coupling coefficient c_j . Note that the classical equations of motion are defined by the Hamiltonian, Eq. 4, using the traceless form of the $\hat{V}(x)$ operator, as shown above.

All the properties of the bath are described entirely by the spectral density. The two most commonly studied spectral densities are the Ohmic and Debye forms, $J_{\text{Oh}}(\omega)$ and $J_{\text{De}}(\omega)$, given by

$$J_{\text{Oh}}(\omega) = \eta \omega \exp\left(-\frac{\omega}{\omega_c}\right) \quad (16a)$$

$$J_{\text{De}}(\omega) = \eta \omega \frac{\omega_c}{\omega^2 + \omega_c^2}, \quad (16b)$$

where ω_c is the characteristic frequency of the bath and η is the coupling strength. In the Ohmic case, the Kondo parameter, $\xi = 2\eta/\pi$, is often used to give the strength of the system-bath coupling instead. It is worth noting that the Debye spectral density spans a frequency range much broader than that of $J_{\text{Oh}}(\omega)$ and, as a result, constitutes a greater numerical challenge.²³

In order to perform numerical simulations it is necessary to discretize the bath into the form

$$J(\omega) = \frac{\pi}{2} \sum_{j=1}^F \frac{c_j^2}{m_j \omega_j} \delta(\omega - \omega_j), \quad (17)$$

for which a number of such schemes have been proposed.^{54–57} In this work, a strategy which reproduces exact values for the reorganization energy was used.^{55,56} The choice of mass, m_j , has no effect on the results.

A set of simulations, calculating the population difference between the two quantum states of the spin-boson Hamiltonian were carried out, using both Ohmic and Debye spectral densities. In each case the calculations were

converged with respect to the number of nuclear degrees of freedom used for the bath discretization.

The phase-space integrals in Eq. 8 were carried out by Monte Carlo importance sampling. Initial conditions for the nuclear modes were drawn from the thermal Wigner distribution of the uncoupled bath,

$$\rho_b^w(x, p) = \prod_{j=1}^F 2 \tanh\left(\frac{1}{2}\beta\omega_j\right) \exp\left[-\left(\frac{p_j^2}{m_j\omega_j} + m_j\omega_j x_j^2\right) \tanh\left(\frac{1}{2}\beta\omega_j\right)\right], \quad (18)$$

where β is the inverse temperature. ρ_{el}^w provides a convenient distribution from which to sample the initial conditions for the mapping variables.²²

The results of the various definitions of the LSC-IVR correlation functions are compared with numerically exact quadiabatic propagator path-integral (QUAPI) calculations.⁴⁶

B. Ohmic bath

The first system chosen corresponds to the intermediate regime between strongly incoherent decay and coherent oscillations and is characterized by moderate system-bath coupling. The particular set of parameters has been extensively studied using a number of different semiclassical dynamics methods.^{41,42} Here, simulations were found to converge with a total of 10^6 trajectories, using a bath of $F = 36$ nuclear degrees of freedom and employing a timestep of $\delta t = 0.01\Delta^{-1}$.

Fig. 1 shows the time-dependent population difference, $P(t)$, as well as the correlation functions from which it was constructed, in accordance with the definitions given in Table I. Notably, both “single SEO” and “double SEO” fail to capture the correct asymptotic limit of $P(t)$. Closer inspection of the constituent correlation functions, $C_{\sigma_z\sigma_z}(t)$ and $C_{\mathcal{I}\sigma_z}(t)$, reveals that while the “double” approach of sampling electronic initial conditions from ϕ^2 performs somewhat better than single” for $C_{\sigma_z\sigma_z}(t)$, any significant errors in $P(t)$ arise from approximations to $C_{\mathcal{I}\sigma_z}(t)$. The “single Wigner” result is an improvement over using the SEO operator, although employing our approach of setting the identity operator to the number 1, is clearly the most accurate of all. Both the “single unity” and “double unity” formulation of the $C_{\mathcal{I}\sigma_z}(t)$ correlation function capture the long-time limit of its decay. As a result the population differences resulting from these two methods yield a drastic improvement over all the other results, with “double unity” in particular yielding close to quantitative accuracy.

To ascertain the general validity of our approach, a second parameter set was investigated for the Ohmic spectral density. Previously studied with a number of methods,⁴¹ this system is characterized by stronger

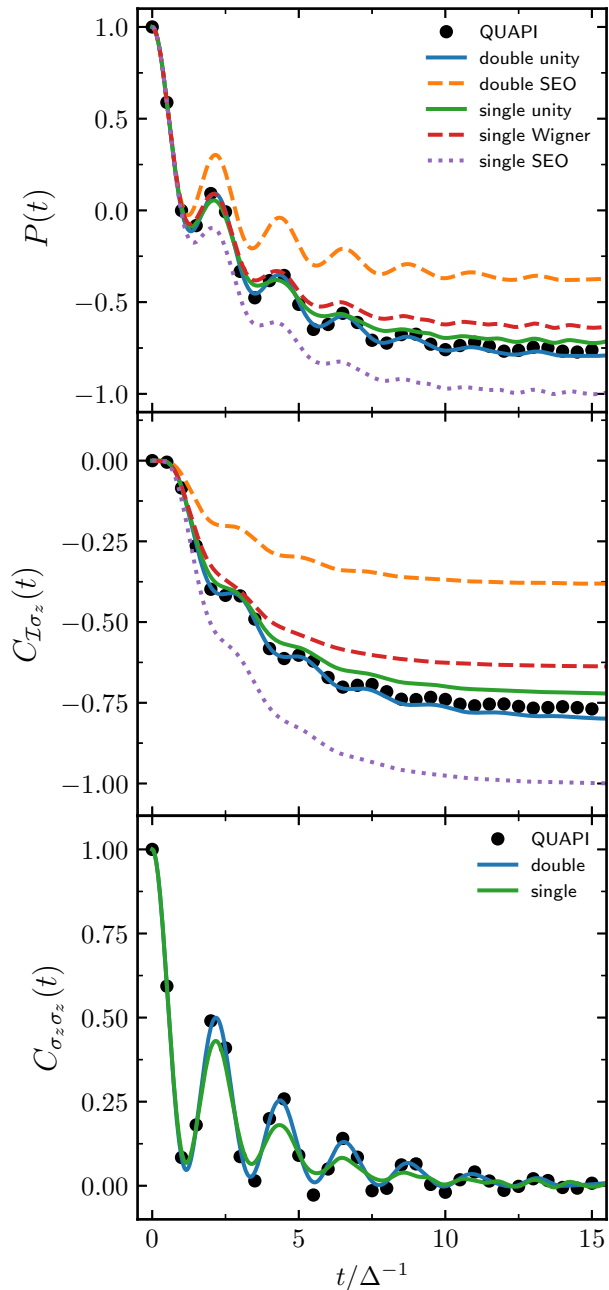


FIG. 1. Time-dependent population difference and the constituent correlation functions obtained using different LSC-IVR definitions for a spin-boson model with an Ohmic bath and parameters $\varepsilon = \Delta$, $\beta = 10\Delta^{-1}$, $\omega_c = 2.5\Delta$ and $\xi = 0.2$. The various approaches are defined in Table I.

system-bath coupling, which in this case results in critical damping. The timestep and convergence parameters were identical to those of the first system.

Fig. 2 shows the population differences, again calculated using the approaches outlined in Table I, for this second parameter set. The accuracy of the different approaches with respect to the exact QUAPI reference re-

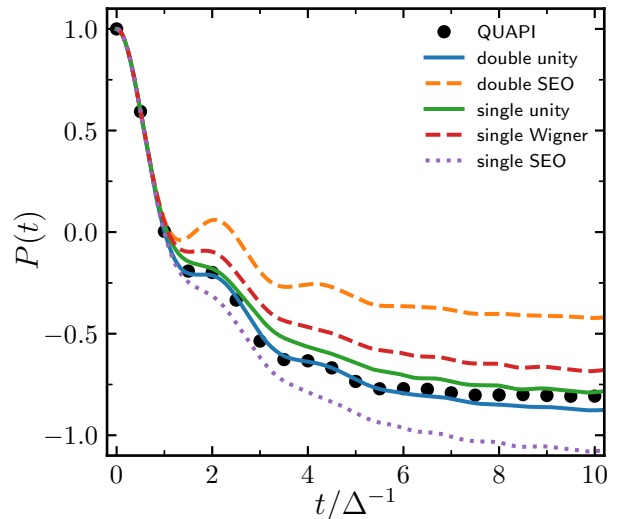


FIG. 2. As top panel of Fig. 1 with parameters $\varepsilon = \Delta$, $\beta = 5\Delta^{-1}$, $\omega_c = 2\Delta$ and $\xi = 0.4$.

sult is very similar to that shown in Fig. 1. “Single SEO” and “double SEO” fail to reach the correct long-time asymptote of the population difference. In addition, with the stronger system-bath coupling present, “double SEO” reports spurious oscillatory structure in the short time limit. It would therefore fail to identify this particular parameter set as resulting in critical damping. Again “single Wigner” yields somewhat better results, and both “single unity” and “double unity”, corresponding to our new strategy of setting the identity equal to 1, considerably outperform all other approaches.

C. Debye bath

As mentioned in Sec. III A, the Debye spectral density is significantly more challenging on account of spanning a broader range of frequencies. Consequently, with the parameters chosen here, results were found to converge using a bath of $F = 60$ nuclear degrees of freedom, averaging over a total of 10^6 semiclassical trajectories with a timestep of $\delta t = 0.0025\Delta^{-1}$. The shorter timestep was required in order to accurately treat the higher frequencies contained in the bath.

The set of parameters chosen represent the most coherent of the three systems reported here, with the weakest system-bath coupling. Results for the time-dependent population difference are shown in Fig. 3. Again, similarly to both Ohmic systems discussed above, the “single SEO” and “double SEO” approaches fail to capture the correct long-time limit of the population difference. “Single Wigner” somewhat improves on this, but our new approach, “double unity,” yields the best results by a significant margin, approaching quantitative accuracy with

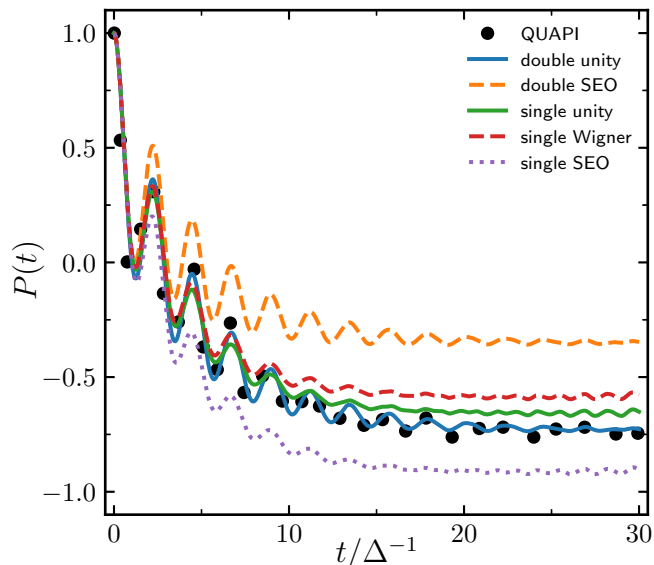


FIG. 3. As top panel of Fig. 1 but with a Debye bath and parameters $\varepsilon = \Delta$, $\beta = 50\Delta^{-1}$, $\omega_c = 5\Delta$ and $\eta = 0.25$. Exact data taken from Ref 43.

respect to the QUAPI benchmark.

IV. CONCLUSION

Based on our study, we propose a simple modification of the standard nonadiabatic LSC-IVR approximation for quantum correlation functions. Wherever possible, the correlation function of interest should be rewritten in terms of Pauli matrices and the identity, and given that the effect of the latter is known to be exactly unity, it should not be estimated by the classical mapping variables, but replaced by its known value, the number 1. Although we have only presented a formulation for dynamical simulation of a two-state system, the mapping approach can be extended to an arbitrary number of electronic states.^{18,19} Also, as it is possible to split any Hermitian operator into a trace-containing and traceless part,²⁰ our strategy is not limited to electronic-state population differences of two-state systems but can also be applied in more general cases.

The benefits associated with this simple strategy have been demonstrated on asymmetric spin-boson models with both Ohmic and Debye spectral densities. In each case, employing the aforementioned representation of the identity operator resulted in a significant improvement in the quality of results. Notably, in comparison to traditional approaches, which predict the wrong asymptotic limit for these systems, our approach consistently yields near quantitative accuracy in the cases investigated in this work.

Note that in principle one can choose different approaches for each of the two correlation functions. It would therefore be possible to calculate a population dif-

ference using the “double” definition of $C_{\sigma_z\sigma_z}(t)$ and the “single unity” $C_{\mathcal{I}\sigma_z}(t)$. For the systems presented here, the result is comparable in accuracy to “double unity”. In future work, we will continue to test these strategies to discover the most reliable strategy.

Different approaches have been previously proposed to address the shortcomings of classical mapping trajectories. For example, methods employing focused sampling³⁶ force the total population to be unity. Note that these cannot therefore benefit further from our strategy. Another example is the symmetrical windowing approach,³⁷ in which binning is used to evaluate the effect of the state operators. Our approach is significantly simpler and has a stronger connection to the original LSC-IVR derivation as well as the formally exact properties of the mapping representation.

The motivation underlying our strategy is similar to that behind work using generalized quantum master equations.^{41–43} Both approaches use exact quantum mechanical information, where possible, to improve the accuracy, or rather avoid the loss in accuracy, of semiclassical trajectories. Notably, the accuracy gain which we demonstrate in this work is similar to what can be achieved using such generalized quantum master equation methods.

Other quantum dynamics methods which utilize the mapping approach may also be able to benefit from employing a similar strategy to that suggested here. These include non-linearized semiclassical dynamics,^{18,21,38,39} partially-linearized density matrix,²⁸ the forward-backward trajectory solution²⁵ of quantum-classical Liouville dynamics,¹⁶ and nonadiabatic ring-polymer molecular dynamics.^{30–35} This study may thus have much wider implications for the methodology development of nonadiabatic dynamics simulations.

ACKNOWLEDGEMENTS

M.A.C.S. would like to acknowledge financial support through the ETH postdoctoral fellowship. The authors also acknowledge the support from the Swiss National Science Foundation through the NCCR MUST (Molecular Ultrafast Science and Technology) Network.

¹R. A. Marcus, *Rev. Mod. Phys.* **65**, 599 (1993).

²D. Chandler, in *Classical and Quantum Dynamics in Condensed Phase Simulations*, edited by B. J. Berne, G. Cicciotti, and D. F. Coker (World Scientific, Singapore, 1998) Chap. 2, pp. 25–49.

³W. Domcke, D. R. Yarkony, and H. Köppel, eds., *Conical Intersections: Electronic Structure, Dynamics and Spectroscopy* (World Scientific, Singapore, 2004).

⁴J. C. Tully, *J. Chem. Phys.* **137**, 22A301 (2012).

⁵H.-D. Meyer, U. Manthe, and L. S. Cederbaum, *Chem. Phys. Lett.* **165**, 73 (1990).

⁶H. Wang and M. Thoss, *J. Chem. Phys.* **119**, 1289 (2003).

⁷X. Chen and V. S. Batista, *J. Chem. Phys.* **125**, 124313 (2006).

⁸G. W. Richings, I. Polyak, K. E. Spinlove, G. A. Worth, I. Burghardt, and B. Lasorne, *Int. Rev. Phys. Chem.* **34**, 269 (2015).

- ⁹M. Ben-Nun and T. J. Martínez, *J. Chem. Phys.* **108**, 7244 (1998).
- ¹⁰M. A. C. Saller and S. Habershon, *J. Chem. Theory Comput.* **11**, 8 (2015); *J. Chem. Theory Comput.* **13**, 3085 (2017).
- ¹¹J. C. Tully, *J. Chem. Phys.* **93**, 1061 (1990).
- ¹²G. Stock, *J. Chem. Phys.* **103**, 1561 (1995).
- ¹³G. Stock and M. Thoss, *Adv. Chem. Phys.* **131**, 243 (2005).
- ¹⁴F. Agostini, A. Abedi, and E. K. U. Gross, *J. Chem. Phys.* **141**, 214101 (2014).
- ¹⁵N. Makri, *Int. J. Quantum Chem.* **115**, 1209 (2015).
- ¹⁶R. Kapral, *J. Phys.-Condens. Mat.* **27**, 073201 (2015).
- ¹⁷X. Tao, P. Shushkov, and T. F. Miller III, *J. Chem. Phys.* **148**, 102327 (2018).
- ¹⁸G. Stock and M. Thoss, *Phys. Rev. Lett.* **78**, 578 (1997).
- ¹⁹H.-D. Meyer and W. H. Miller, *J. Chem. Phys.* **70**, 3214 (1979).
- ²⁰A. Kelly, R. van Zon, J. Schofield, and R. Kapral, *J. Chem. Phys.* **136**, 084101 (2012).
- ²¹X. Sun and W. H. Miller, *J. Chem. Phys.* **106**, 6346 (1997).
- ²²X. Sun, H. Wang, and W. H. Miller, *J. Chem. Phys.* **109**, 7064 (1998).
- ²³H. Wang, X. Song, D. Chandler, and W. H. Miller, *J. Chem. Phys.* **110**, 4828 (1999).
- ²⁴H. Kim, A. Nassimi, and R. Kapral, *J. Chem. Phys.* **129**, 084102 (2008).
- ²⁵C.-Y. Hsieh and R. Kapral, *J. Chem. Phys.* **137**, 22A507 (2012); *J. Chem. Phys.* **138**, 134110 (2013).
- ²⁶U. Müller and G. Stock, *J. Chem. Phys.* **108**, 7516 (1998).
- ²⁷S. Bonella and D. F. Coker, *J. Chem. Phys.* **122**, 194102 (2005).
- ²⁸P. Huo and D. F. Coker, *J. Chem. Phys.* **135**, 201101 (2011).
- ²⁹N. Ananth and T. F. Miller III, *J. Chem. Phys.* **133**, 234103 (2010).
- ³⁰J. O. Richardson and M. Thoss, *J. Chem. Phys.* **139**, 031102 (2013).
- ³¹J. O. Richardson, P. Meyer, M.-O. Pleinert, and M. Thoss, *Chem. Phys.* **482**, 124 (2017), arXiv:1609.00644 [physics.chem-ph].
- ³²N. Ananth, *J. Chem. Phys.* **139**, 124102 (2013).
- ³³J. R. Duke and N. Ananth, *J. Phys. Chem. Lett.* **6**, 4219 (2015).
- ³⁴T. J. H. Hele and N. Ananth, *Faraday Discuss.* **195**, 269 (2016).
- ³⁵S. N. Chowdhury and P. Huo, *J. Chem. Phys.* **147**, 214109 (2017), arXiv:1706.08403 [physics.chem-ph].
- ³⁶S. Bonella and D. F. Coker, *J. Chem. Phys.* **118**, 4370 (2003).
- ³⁷S. J. Cotton and W. H. Miller, *J. Chem. Phys.* **139**, 234112 (2013); W. H. Miller and S. J. Cotton, *Faraday Discuss.* **195**, 9 (2016).
- ³⁸M. Thoss and G. Stock, *Phys. Rev. A* **59**, 64 (1999); M. Thoss, W. H. Miller, and G. Stock, *J. Chem. Phys.* **112**, 10282 (2000).
- ³⁹M. S. Church, T. J. Hele, G. S. Ezra, and N. Ananth, *J. Chem. Phys.* **148**, 102326 (2018).
- ⁴⁰Q. Shi and E. Geva, *J. Chem. Phys.* **119**, 12063 (2003).
- ⁴¹A. Kelly, N. Brackbill, and T. E. Markland, *J. Chem. Phys.* **142**, 094110 (2015).
- ⁴²A. Kelly, A. Montoya-Castillo, L. Wang, and T. E. Markland, *J. Chem. Phys.* **144**, 184105 (2016).
- ⁴³A. Montoya-Castillo and D. R. Reichman, *J. Chem. Phys.* **144**, 184104 (2016).
- ⁴⁴A. Montoya-Castillo and D. R. Reichman, *J. Chem. Phys.* **146**, 084110 (2017).
- ⁴⁵W. H. Miller, *J. Phys. Chem. A* **105**, 2942 (2001).
- ⁴⁶N. Makri, *Chem. Phys. Lett.* **193**, 435 (1992).
- ⁴⁷A. Garg, J. N. Onuchic, and V. Ambegaokar, *J. Chem. Phys.* **83**, 4491 (1985).
- ⁴⁸A. J. Leggett, S. Chakravarty, A. T. Dorsey, M. P. A. Fisher, A. Garg, and W. Zwerger, *Rev. Mod. Phys.* **59**, 1 (1987).
- ⁴⁹U. Weiss, *Quantum Dissipative Systems*, 4th ed. (World Scientific, Singapore, 2012).
- ⁵⁰C. H. Mak and D. Chandler, *Phys. Rev. A* **44**, 2352 (1991).
- ⁵¹D. E. Makarov and N. Makri, *Phys. Rev. A* **48**, 3626 (1993).
- ⁵²M. Topaler and N. Makri, *J. Phys. Chem.* **100**, 4430 (1996).
- ⁵³M. Thoss, H. Wang, and W. H. Miller, *J. Chem. Phys.* **115**, 2991 (2001).
- ⁵⁴U. Müller and G. Stock, *J. Chem. Phys.* **111**, 77 (1999).
- ⁵⁵H. Wang, M. Thoss, and W. H. Miller, *J. Chem. Phys.* **115**, 2979 (2001).
- ⁵⁶I. R. Craig, M. Thoss, and H. Wang, *J. Chem. Phys.* **127**, 144503 (2007).
- ⁵⁷I. R. Craig and D. E. Manolopoulos, *J. Chem. Phys.* **122**, 084106 (2005).